DOI:10.13656/j.cnki.gxkx.2004.04.014
广西科学 Guangxi Sciences 2004, 11 (4) 327331

Studies on the Reaeration Process of Turbulent Water
紊动水体中气液传质过程分析

Zhang Zongcai Zhang Xinshen Dai Hong Zhang Mingrang
张宗才 张新申 代 红 张铭让

(Key Laboratory of Leather Chemistry and Engineering (Sichuan University), Ministry of Education, Chengdu, Sichuan, 610065, China)
(皮革化学与工程教育部重点实验室(四川大学) 四川成都 610065)

Abstract The dissolved oxygen concentration in the water body is one of the most important indicators that can be used to evaluate the water body polluted by organic matter. The reaeration process and reaeration velocity play key roles in the transfer, diffusion and purification process of organic pollutants. This paper describes researches on the reaeration process of turbulent water body as well as the effect of neutral salts and organics in turbulent water on the reaeration of experimental scale. The relationship between the reaeration coefficient k_2 and water depth H is simulated and calculated based on the analysis of interfacial mass transfer coefficient.

Key words reaeration, dissolved oxygen, turbulent, mass transfer

摘要 在实验水槽中,通过测量水体中溶解氧浓度的变化,研究不同搅拌速度、搅拌头处于不同水深情况下的复氧过程,以及紊动水体中中性盐和有机物对复氧的影响,并在表面传质系数分析的基础上,摸拟计算复氧系数 k_2 与水深 H 的关系。结果表明,水体内溶解氧量不仅取决于水气介面传质速率,而且也与水体内氧的扩散有关,紊动水体的复氧过程更与表面紊动动能有关;中性盐的存在对复氧影响较小,而葡萄糖则明显降低复氧速度。

关键词 复氧 溶解氧 紊动 传质
中图法分类号 Q375.5

The reaeration process is a gas-liquid mass transfer process. To measure the reaeration velocity, the gas-liquid mass transfer coefficient k_2 and surface mass transfer coefficient K_L are presented[1]. The progress of studies on the theory of gas-liquid mass transfer is restricted by the experimental technology. Therefor, the experimental simulations of gas-liquid mass transfer are not sufficient. For practical purposes, the value of reaeration coefficient k_2 is generally taken to be the empirical or semi-empirical formulas which are based on the correlation between k_2 and specific parameters such as velocity of flow, depth of water and hydraulic gradient[2]. Besides, these comparison expressions are not popularly applicable because of the complexity of bottom and boundary of natural rivers.

The reaeration process from atmosphere is usually extremely complex, and classical mass transfer theory assume this procedure to be a simple and ideal procedure[3]. The structure of the flow field of interface is neglected, but the practical research indicates that the reaeration process involves the thermodynamic property and dynamics property of the interface region[4,5].

1 Experiment

Reaeration test is carried out in a cylinder glass bucket with ϕ30cm$\times$40cm in dimension. A mixer with a plate mixing head (5cm$\times$1.5cm) is installed in the bucket. Dissolved oxygen is measured with HANNA HI9143 portable dissolved oxygen meter that the measuring resolution is 0.01mg/L O_2.

The right amount of tap water is infused into the bucket before the test, and a definite quantity of Na_2SO_3 and a little catalyst $CoCl_2$ are added for making up a loss of oxygen in water. The test is started when the dissolving oxygen in water is below 0.5 mg/L. The dissolved oxygen levels are recorded at $t=0$ min at a given stirring speed. Dis-

2004-05-27 收稿, 2004-07-12 修回。

solved oxygen records are collected at different measuring positions at intervals of definite time (see Figure 1). Dissolved oxygen values are determined with mixers of 50rpm and 200rpm, and the mixer headers are placed in the surface layer (3cm from surface), in the middle layer (18cm from surface) and in the bottom layer (33cm from surface) of the water body respectively.

At low rotational speeds, circulation flow obviously occurs in the fracture layer where the mixer headers are located. The speed of circulation flow is comparatively slowed down by friction of the wall near the rim of the tank. At high rotational speeds, there occurs significant eddy flow besides circulation flow, thus the osmosis and intermixing of particles of liquid are augmented, the conversation and transfer of momentum of water body are enhanced and the homogenizing of distribution of current velocity increases.

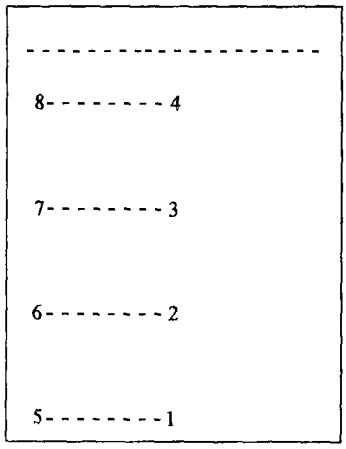

Fig. 1 A sketch map of measuring points of the device

2 Reaeration Rule of Turbulent water

2.1 Analysis of turbulent kinetic energy of turbulent water

As variations of the vertical velocity of flow are significantly related to the variations of wall resistance caused by the tank rim, Reynolds criterion (Re) is presented as

$$Re = \frac{d_m^2 n \rho}{\mu}, \tag{1}$$

Where

d_m = length of the header of mixer, cm;

n = number of revolution, rpm;

ρ = fluid specific density;

μ = fluid viscosity.

In terms of Boundary Laminar Theory, the thickness of laminar is a function of Reynolds criterion (Re), as follows:

$$\delta \propto \frac{1}{\sqrt{Re}}. \tag{2}$$

Applied to the calculation of the laminar flow of boundary layer, Rice-Stock's formula[5] can be rounded off to the following equation because water viscosity and vertical current are so small that they can be neglected.

$$u_x = \frac{\partial u_x}{\partial x} + u_y \frac{\partial u_y}{\partial y} = -\frac{1}{\rho}\frac{\mathrm{d}p}{\mathrm{d}x} + \frac{\mu}{p}\frac{\partial^2 u_x}{\partial y^2}. \tag{3}$$

The variation of vertical velocity along the water depth is both related to the number of revolution and the location of the mixer header. In general, this variation is small. As the mixer header is located in the surface layer of the water body, turbulent kinetic energy is large. But the kinetic energy reduces significantly as water depth increases. Thus, the variation of kinetic energy along the water depth is significant. As the mixer header is located in the bottom layer or in the middle layer of the water body, the variation of kinetic energy along the water depth is less significant although the kinetic energy reduces.

2.2 Surface mass transfer coefficient of turbulent water

According to the Law of Energy Conservation, the amount of the dissolved oxygen transferring from air-water free surface into the water body per unit time equals the incremental amount of dissolved oxygen in the water body. This relationship can be expressed by the equation

$$\int_0^A \int_0^t F \mathrm{d}t \mathrm{d}A = \int_0^A \int_0^t K_L (C_s - C_1) \mathrm{d}t \mathrm{d}A = \int_0^\Omega \int_{C_0}^{C_t} \mathrm{d}C \mathrm{d}\Omega. \tag{4}$$

First, after the discreteness of the equation, we apply average of surface mass transfer coefficient to this equation and rearrange the left part of this formula as following

$$K_L \sum_{i=1}^{M_1} \{ \Delta A_i \sum_{n=0}^{N-1} [(C_s - C_{1i}^n) \Delta t_n] \}, \tag{5}$$

C_{1i}^n denotes the concentration value at time n, at sample point i in the surface layer of the water body, whereas M_1 denotes the sample point number in the surface layer of the water body. The right part of this formula is expressed as:

$$\sum_{i=1}^{M} [(C_i^n - C_i^0) \Delta \Omega_i], \tag{6}$$

where M denotes the sample point number of the dissolved oxygen in the reaeration water body, C_i^n is the concentration value at time n, at sample point i.

Now, we get the expression of surface mass transfer coefficient

$$K_L = \frac{\sum_{i=1}^{M}[(C_i^n - C_i^0)\Delta\Omega_i]}{\sum_{i=1}^{M_1}\{\Delta Ai\sum_{i=0}^{N-1}[(C_s - C_{1i}^n)\Delta t_n]\}}. \quad (7)$$

With mixing, the specific area of air-water interface increases when eddy flow occurs in the surface layer of the water body, and the gas near the interface is involved or inhaled into the centre of water body because the eddy flow is due to the turbulent fluctuation of the water body. Thus the process of oxygenation is accelerated in the surface layer of the water body.

In terms of Fick's Law of Diffusion, the dissolved oxygen concentration is related both to turbulent kinetic energy and to oxygen concentration in the water body near the air-water interface.

$$F_t = f(k, c), \quad (8)$$

express the surface mass transfer coefficient of turbulent water in the form of an equation

$$K_L = Ak_0^n + k_{LO}. \quad (9)$$

Li Ran and his cooperators[6] rounded off the tank experiments and calculations with the relational expression between surface mass transfer coefficient of turbulent water and turbulent kinetic energy, as follows:

$$K_L = 0.085k^{1/2} + 0.0014. \quad (10)$$

2.3 Analysis of results of the experiments of dissolved oxygen in turbulent water

In experimental tanks, the results of the dissolved oxygen at different conditions of rotational speeds and locations of mixer header are expressed in Figures 2 to 4.

As illustrated in Figures 2 and 3, an increase in rotational speed results in an increase in reaeration rate and reaeration coefficient. Rotational speed variations in the surface layer have much more significant effect on reaeration coefficient variations than rotational speed variations in the bottom layer. The rotational speed in the bottom layer increased by three times, and the coefficient is raised by 19 percent. Whereas, the rotational speed in the surface layer increased by three times, and the coefficient is raised by 259 percent.

The change of dissolved oxygen concentration vertical distribution of turbulent water body is less than that of a stable water body. Furthermore, with the mixing in the surface layer, the faster the rotation is, the more the turbulent kinetic energy is; the more the increase of the dissolved oxygen is, the less the vertical concentration gradient is. This demonstrates that the turbulence accelerates the diffusion of dissolved oxygen. Also, the reaeration process is at a faster rate particularly as the turbulent kinetic energy increases.

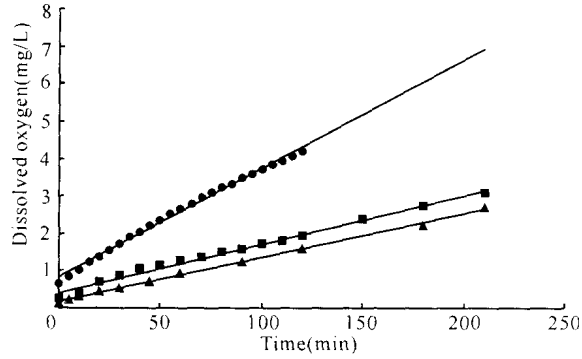

Fig. 2 Reaeration processes at the different mixing speeds in the bottom layer of water body (water depth is 33cm)

—●—: high speed (500rpm); —■—: medium speed (200rpm); —▲—: low speed (50rpm).

It is particularly true from Figure. 3 that the faster the rotation is, the faster the reaeration process is. At the condition of fast mixing, the reaeration value exceeds 4mg/L within 50 minutes, whereas at the condition of 100rpm, the reaeration value is below 4mg/L.

However, the faster the rotation is, the more the energy consumption is. Therefore, the rotational speed is feasibly reduced and an optimum rotational speed with characters of meeting the requirements of efficient and energy consumption is available for practical purpose.

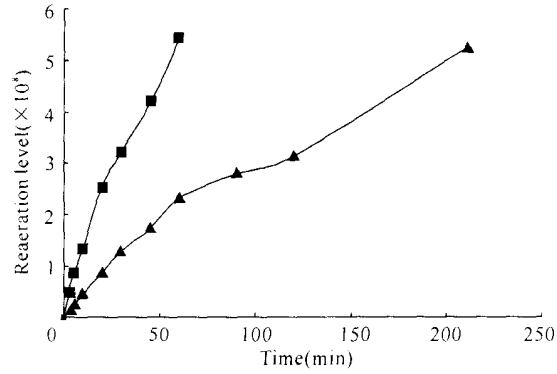

Fig. 3 Reaeration processes in the surface layer of the water body (water depth is 33cm)

—■—: fast surface stirring (500rpm); —▲—: surface stirring (100rpm).

2.4 Reaeration at different water depths in low speed

As shown in Figures 4, surface aeration affects reaeration process effectively, compared to internal aeration and bottom aeration. The reaeration value almost reaches 4mg/L within 150 minutes at the conditions of surface aeration, whereas the value representing internal aeration reaches about 2mg/L and the value representing bottom aeration drops to 1.5mg/L within the 150minutes. Furthermore, the curve of internal aeration is particularly similar to that of bottom aeration, while the curve of surface aeration keeps successively increasing. Experimental investigations demonstrate the surface aeration is relatively suitable for the operation.

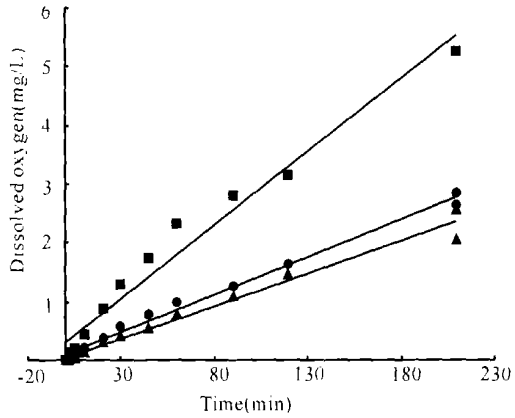

Fig. 4 Reaeration processes at the different water depths under slow mixing (rotational speed is 50rpm)

—■—: surface; —●—: middle section; —▲—: bottom.

In addition, experimental investigations show the rate of increase of dissolved oxygen in the water body is related to the initial value of oxygen defection if the rotational speed remains constant. The less the oxygen defection is, the slower the increase of dissolved oxygen is, which probably accounts for the buffer phenomenon of the reaeration process. That is, the reductive matter added into the water body to improve the initial value of oxygen defection is not completely consumed, which leads to the consumption of oxygen in the early stage.

Contrasts and analysis are performed in different reaeration coefficients (different water depths, same rotational speed) to ascertain the close relationship between reaeration coefficient k_2 and water depth H. It is shown that K_L is a function of H. Applying Equation (9) and rearranging the expression, we get

$$k_2 = A \cdot H^{1/n} + B. \quad (11)$$

As illustrated in Figures 5, k_2 can be expressed by a linear function of 1/3 power of H, as follows

$$k_2 = 133.036H^{1/3} - 0.01872. \quad (12)$$

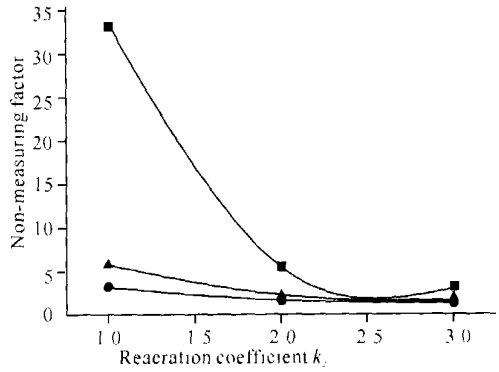

Fig. 5 Relationship between water depth and reaeration coefficient

—■—: YH; —▲—: $1/H^{1/2}$; —●—: $1/H^{1/3}$.

2.5 Effects of neutral salt and organic matter of the water body on the reaeration process

In the trial, 1g/L potassium chloride, 0.5g/L urea and 0.5g/L glucose are added into the water body respectively, the results are illustrated in Figure 6.

Figure 6 indicates that neutral salt added contributes little to the reaeration of the water body, whereas glucose added results in obvious drop as linear changes. If there exists organic matter glucose, the restoring of dissolved oxygen is relatively slow, which probably accounts for the chemical reaction of dissolved oxygen with glucose. If there exists salt and urea, the restoring of dissolved oxygen is affected slightly.

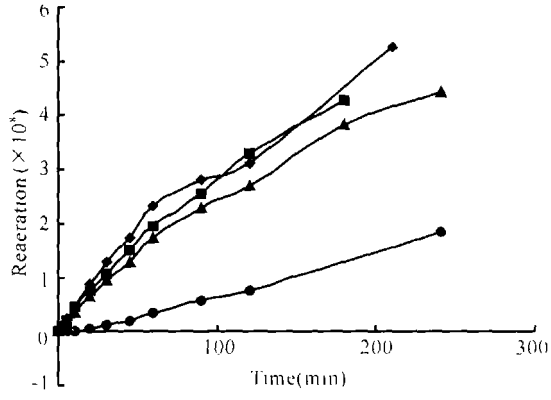

Fig. 6 Effects of neutral salt and organic matter of the water body on the reaeration process

—◆—: top water, —■—: 1 g/L KCl solution; —▲—: 1 g/L KCl + 0.5g/L urea solution; —●—: 0.5 g/L glucose solution.

3 Conclusion

Based on the trials of reaeration of turbulent water and

theoretic analysis on the turbulent kinetic energy and interfacial mass transfer coefficient of turbulent water, the conclusions are as follows.

(Ⅰ)The results of reaeration trials of water body show that dissolved oxygen level in water body is related not only to liquid-gas interface mass transfer ratio, but also to diffusion within water body.

(Ⅱ)Surface reaeration process of turbulent water is dependent on surface turbulent kinetic energy (or turbulent state), advancing oxygen in air contact with water by eddy flow and promoting the air drawn/inhaled into water near interface. Oxygen diffusion and distrbution in water is put forward by the concept of oxygen-penetration.

(ⅢD)Neutral salts have few effect on the reaeration of water. But reaeration ratio of water dropped obviously when glucose is added into water.

Reference

1 Atkinson J F, Blair S, Taylor S, et al. Surface aeration. Journal of Environmental Engineering, 1995, 121(1): 113118.

2 Lewis W K, Whitman W C. Principles of gas absorption. Industrial and Engineering Chemistry, 1924. 16.

3 Ma Youguang, Bei Pong, Yu Guozong. Research progress in gas-liquid mass transfer theory. Chemical Engineering(China), 1996, 24(6): 711.

4 Ma Youguang, Song Baole, Yu Guozong. Interface property on gas-liquid mass transfer. Chemical Engineering(China), 1997, 25(4): 67, 20.

5 Shanghai College of Chemical Engineering, et al. Chemical Engineering. Beijing: Chemical Engineering Press, 1980.

6 Li Ran, Li Jia, Zhao Wenqian, et al. Study on reaeration laws of turbulent water body. ACTA Scientian Circumstantiae, 2000, 20(6): 723726.

(责任编辑: 蒋汉明　邓大玉)

(上接第 326 页 Continue from page 326)

25 Dehouche Z, Djiaozandry R, Goyette J, et al. Evalution Techniques of cycling effect on the remodynamic and crystal structure properties of Mg_2Ni alloys. Journal of Alloys and Compands, 1999, (288): 269276.

26 周怀营, 王仲民, 顾正飞, 等. Preparation and structure of $Mg_{2-x}Re_xNi$(where Re= La, Ce, Pr, Nd, Y). 中国稀土学报, 2004, 22: 263267.

27 Dehouche Z, Djiaozandry R, Goyette J, et al. Evalution techniques of cycling effect on the remodynamic and crystal structure properties of Mg_2Ni alloys. Journal of Alloys and Compands, 1999, (288): 269276.

28 Song M Y. Phase separation of Mg_2Ni by hydriding dehydriding cycling. Journal of Alloys and Compands, 1999, (282): 297301.

29 Kadir K, Noreus D, Yamashita I. Structure determination of $AMgNi_4$(where A= Ca, La, Ce, Pr, Nd and Y) in the $AuBe_5$ type structure. Journal of Alloys and Compounds, 2002, (345): 140143.

30 Werner P E, Eriksson L. World Directory of Powder Diffraction Programs. Release, 1993, 2. 12.

31 Aono K, Orimo S, Fujii H. Structural and hydriding properties of $MgYNi_4$: A new intermetallic compound with $C_{15}b$-type Laves phase structure. Journal of Alloys and Compounds, 2000, (309): 14.

32 Kadir K, Sakai T, Uehara I. Synthesis and structure determination of a new series of hydrogen storage alloys; RMg_2Ni_9 (R= La, Ce, Pr, Nd, Sm and Gd) built from $MgNi_2$ Laves-type layers alternating with AB_5 layers. J Alloys and Comp, 1997, 257: 115121.

33 Wang Z M, Zhou H Y, Gu Z F, et al. Preparation Preparation of $LaMgNi_4$ alloy and its electrode properties. J Alloys and compounds, 2004, 377: 79.

34 Wang Z M, Zhou H Y, Cheng G, et al. Preparation and electrode properties of new ternary alloys: $REMgNi_4$ (RE= La, Ce, Pr, Nd). Alloys and Compounds, 2004, 384: 279282.

35 王仲民. 添加稀土元素对 Mg_2Ni 储氢合金的结构和性能的影响. 稀有金属, 2004, 28(1): 108111.

36 Gennari F C, Urretavizcaya G, Andrade Gamboa J J, et al. New Mg-based alloy obtained by mechanical alloying in the Mg-Ni-Ge system. Joural of Alloys and Compounds, 2003, (354): 187192.

37 Meng Mianwu, Liu Xinyu, Jun Cheng, et al. Electrochemical characteristics of the $Mg_{1-x}La_xNi$ (x= 0, 0. 05, 0. 10) alloy synthesized by mechanical alloying. Joural of Alloys and compounds, 2004, 372, 285289.

(责任编辑: 邓大玉)